

*Electronic Supplementary Information*

**Charge Instability of Symmetry Broken Dipolar States  
in Quadrupolar and Octupolar Triphenylamine  
Derivatives**

**Shanmugam Easwaramoorthi,<sup>\*a,b</sup> Pichandi Thamaraiselvi,<sup>a</sup> Kumaraguru Duraimurugan,<sup>c</sup> Arockiam Jesin Beneto,<sup>c</sup> Ayyanar Siva\*<sup>c</sup> and Balachandran Unni Nair<sup>a</sup>**

<sup>a</sup> *Chemical Laboratory, CSIR-Central Leather Research Institute, Adyar, Chennai, India Fax:91-44-24411630; Tel:91-44-24411630; E-mail: [moorthi@clri.res.in](mailto:moorthi@clri.res.in)*

<sup>b</sup> *CSIR-Network of Institutes for Solar Energy (NISE)*

<sup>c</sup> *Department of Inorganic Chemistry, Madurai Kamaraj University, Madurai, India. E-mail: [drasiva@gmail.com](mailto:drasiva@gmail.com)*

## Discussion

The molecular orbitals of TPA derivatives were calculated using Gaussian 09 at B3LYP/6-31G+(d, p) level of theory and is given in Figure S11. The input files for the TD-DFT calculations were obtained using the optimized geometries at the same level of theory. As can be seen in Figure S11, the HOMO of **dCN** and **tCN** are stabilized respectively by the magnitude of 0.41 and 0.77 eV when compared to that of **mCN**. Similarly, the LUMO also gets stabilized when increasing the number of cyano-substituents from one to three. While the electron density are delocalized over all the phenyl groups irrespective of the substituent in HOMO, the LUMO show significant changes in the localization of electron density with respect to the number of cyano-substituents. Indeed, all the molecules studied here have the electron density localized mostly on the cyanophenyl ring in LUMO. This feature suggests that there is a possibility for the intramolecular charge transfer interactions where the amino group acts as a donor and the cyanophenyl fragment acts as an acceptor. However, it should be noted that the frontier orbitals are not well separated as observed for the molecular dyads showing complete charge transfer, but rather, states which undergo electron density redistribution from donor fragment to the acceptor fragment. To explore further, we have performed the natural transition orbital (NTOs) analysis to understand the nature of the excited states using Gaussian 09 at B3LYP/6-31G+(d, p) level.<sup>S1</sup> This method offers most compact representation of the transition density between the ground and excited states in terms of an expansion into hole and electron states for each given excitation. Natural transition orbitals of the first excited state depicted in Table S5 suggests the pronounced intramolecular charge transfer occurs within the chromophore upon photoexcitation. As expected, the electron density of the hole for **mCN** and **dCN** is delocalized over the aminophenylene moiety without the cyano substitution. Upon excitation the charge is shifted to the cyanophenylene moiety. On the other hand, **tCN** being highly symmetric with all the phenyl ring substituted with cyano group, amino group and one of the cyanophenylene ring acts a donor moiety and the remaining two cyanophenylene moieties acts as an acceptor.

## EXPERIMENTAL PROCEDURE

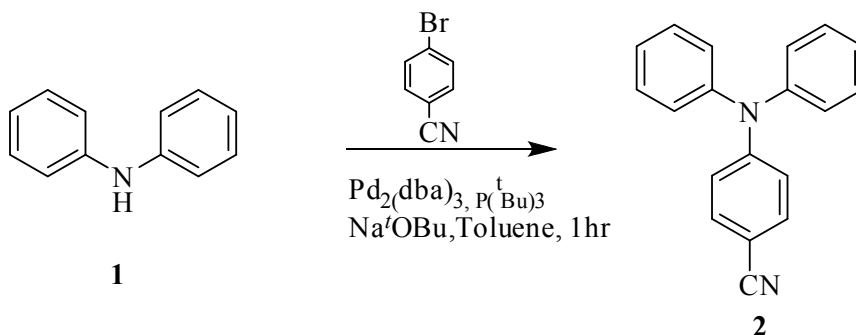
### Materials And Methods

All the chemicals and reagents used in this work were analytical grade. Triphenylamine, was obtained from Alfa Aesar, copper(II)nitrate, diphenylamine, aniline, *p*-aminobenzonitrile and *p*-aminobenzonitrile were obtained from Sigma Aldrich and acetic anhydride was obtained from Merck. The melting points were measured in open capillary tubes and are uncorrected.

The  $^1\text{H}$ , and  $^{13}\text{C}$  NMR spectra were recorded on a Bruker (Avance) 400 MHz and 300 MHz NMR instrument using TMS as internal standard and  $\text{CDCl}_3$  as a solvent. Chemical shifts are given in parts per million ( $\delta$ -scale) and the coupling constants are given in Hertz. Silica gel-G plates (Merck) were used for TLC analysis with a mixture of n-hexane and ethyl acetate as an eluent. Column chromatography was carried out with silica gel (60-120 mesh) using n-hexane and ethyl acetate as an eluent. FT-IR was recorded in a JASCO FT/IR-410 spectrometer. UV-visible absorption spectra were measured using Shimadzu UV-1800 spectrophotometer. The steady state fluorescence measurements were measured using Varian Cary Eclipse fluorescence spectrophotometer. Fluorescence quantum yields were obtained by using fluorescein in 0.05 M  $\text{H}_2\text{SO}_4$  as a standard (0.547). Fluorescence lifetimes were measured by the time correlated single photon counting method. The fluorescence decay curves are measured by exciting the molecules at 375 nm, < 200 ps light using Nano LED. Single crystal X-ray structures were determined using Bruker Kappa APEXII single crystal X-ray diffractometer, at SAIF, IIT-Madras.

### Preparation of (4-cyanophenyl)diphenylamine (mCN):

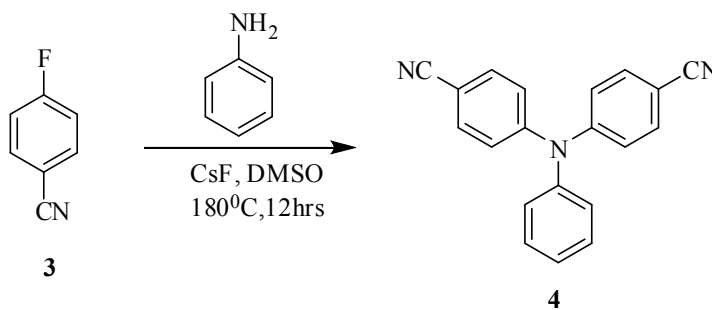
The reaction was carried out with Diphenylamine (170mg, 1mmol) and 4-bromo benzonitrile (188mg, 1.2mmol) with  $\text{Pd}_2(\text{dba})_3$  (92mg, 0.1mmol) and tri-*tert*-butylphosphine (16mg, 0.08mmol) in Na<sup>t</sup>OBu (184mg, 1.5mmol) and toluene (5ml). This mixture was kept stirring for about 1 hour. After one hour the reaction mixture was adsorbed onto the silica gel and chromatographed with 5% ethyl acetate in hexane. The product is an off-white solid. Yield is 130 mg (48%). mp-126-127°C IR (KBr): $\nu$ = 2210 $\text{cm}^{-1}$ ,  $^1\text{H-NMR}$  (300MHz,  $\text{CDCl}_3$ )  $\delta$ =7.733-7.403(d,2H), 7.362-7.310(t,4H), 7.184-7.133(t,4H), 6.976-6.946(dd,4H,J=6Hz).  $^{13}\text{C-NMR}$  (300MHz,  $\text{CDCl}_3$ )  $\delta$ =151.6, 145.9, 133.1, 129.7, 126.1, 125.1, 119.7,104



**Scheme 1:** Preparation of (4-cyanophenyl)diphenylamine

### Preparation of 4,4'-dicyanotriphenylamine (dCN):

The mixture of aniline (0.5 g, 5.37mmol), 4-fluorobenzonitrile (1.3 g, 10.7 mmol), finely grounded cesium fluoride (1.63 g, 10.7 mmol) and 15 ml of DMSO were taken in a inert atmosphere and heated for about 12 hours at 180°C. Then it was cooled to RT and poured into water and extracted with ethylacetate (50ml). The organic layer was washed with brine solution, dried over Na<sub>2</sub>SO<sub>4</sub> and evaporated. The crude product was purified by silica gel (60-120) column chromatography using DCM as an eluent. The product is a pale yellow solid. Yield is 135 mg (10%). mp-191-192°C, IR (KBr):(ν)=2221cm<sup>-1</sup>, <sup>1</sup>H NMR (300MHz, CDCl<sub>3</sub>) δ=7.712-7.683(d,4H), 7.544-7.515(d,4H), 7.425-7.374(t,1H), 7.425-7.314(d,2H), 7.123-7.101(d,4H). <sup>13</sup>C NMR (300MHz, CDCl<sub>3</sub>) δ=159.6, 150.1, 134.4, 133.5, 130.2, 126.9, 126.4, 122.8, 119.6, 118.8, 108.0.



### Preparation of 4,4',4''-Tricyanodiphenylamine (tCN):

*p*-fluorobenzonitrile (0.5 g, 4.12 mmol) and *p*-aminobenzonitrile (487 mg, 4.12 mmol) were dissolved in 10 ml of DMSO. The mixture was stirred for 4 hours at room temperature. Then the reaction mixture was poured into water, precipitate was formed. Filtered and washed with water, dried under vacuum. The crude product was treated with 4-fluorobenzonitrile (386 mg, 3.19 mmol) and  $K_2CO_3$  (882 mg, 6.39 mmol) in 10ml of DMSO. The reaction was heated at 110°C and maintained for about 12 hours. Then it was cooled to room temperature, quenched with water and extracted with chloroform (50ml). The organic layer was separated and washed with brine solution, dried over  $Na_2SO_4$  and evaporated. The crude product was purified by silica gel (60-120mesh) column chromatography using DCM as an eluent. The product is pale pink color. Yield is 120mg (12%) IR (KBr): $\nu$ =2215 $cm^{-1}$ ,  $^1H$  NMR(300MHz,  $CDCl_3$ )  $\delta$ =7.623-7.594(d, 6H), 7.167-7.138(d,6H).  $^{13}C$  NMR (300MHz,  $CDCl_3$ )  $\delta$ =153.6, 145.8, 140.3, 130.0, 126.6, 125.5, 118.2.

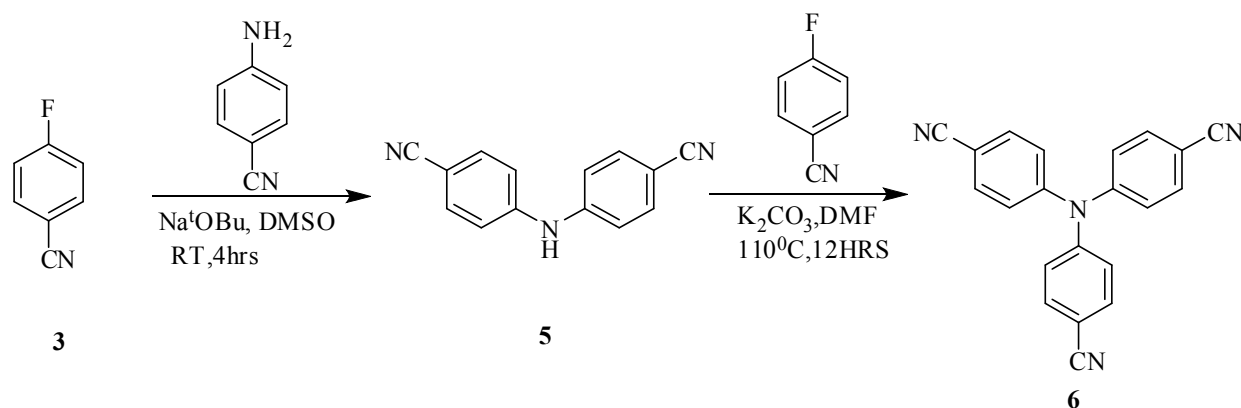


**Table S1** Crystallographic details of compounds **mCN** and **tCN**

	<b>mCN</b>	<b>tCN</b>
<b>Empirical Formula</b>	C <sub>19</sub> H <sub>14</sub> N <sub>2</sub>	C <sub>21</sub> H <sub>12</sub> N <sub>4</sub>
<b>Formula Weight</b>	270.32	320.35
<b>Crystal System</b>	Monoclinic	Orthorhombic
<b>Crystal Size (mm)</b>	0.35 x 0.30 x 0.30	0.35 x 0.30 x 0.30
<b>Space group</b>	P21/c	Pbcn
<b>a/Å</b>	12.2021(6)	8.1650(4)
<b>b/Å</b>	11.4270(6)	11.6360(5)
<b>c/Å</b>	10.8496(6)	17.5650(8)
<b>α/Å</b>	90	90
<b>β/Å</b>	99.451(2)	90
<b>γ/Å</b>	90	90
<b>V/Å<sup>3</sup></b>	1492.26(14)	1668.81(13)
<b>Z</b>	4	4
<b>ρ<sub>calcd</sub>/g cm<sup>-3</sup></b>	1.203 Mg/m <sup>3</sup>	1.275 Mg/m <sup>3</sup>
<b>F(000)</b>	568	664
<b>Temperature (K)</b>	293	293
<b>Radiation MoKα λ/ Å</b>	0.71073	0.71073
<b>Goodness of fit on F<sup>2</sup></b>	1.035	1.048
<b>Number of reflections measured</b>	13606	7581
<b>Number of reflections used</b>	2618	1466
<b>Number of refined parameters</b>	191	117
<b>R<sub>int</sub></b>	0.0266	0.0220
<b>CCDC No.</b>	963776	963777

**Table S2 Selected transitions obtained from TD-DFT calculation at B3LYP/6-31+G (d,p) level**

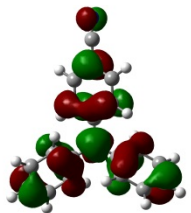
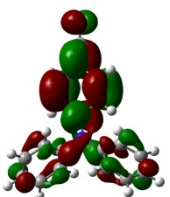
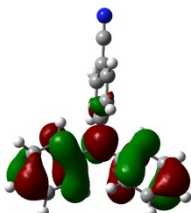
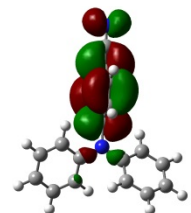
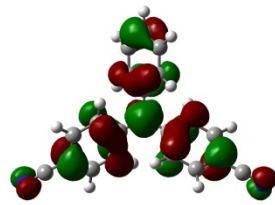
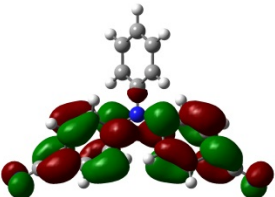
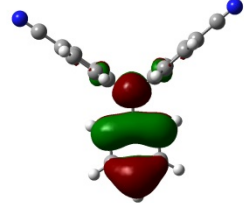
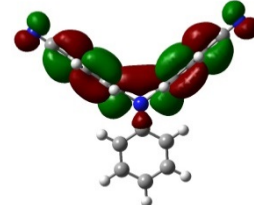
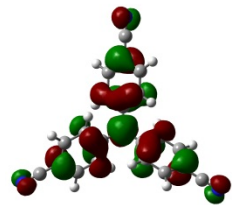
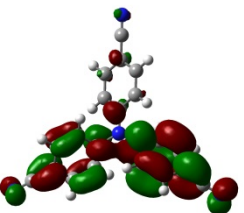
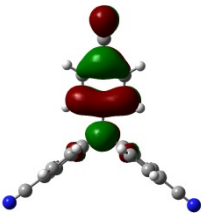
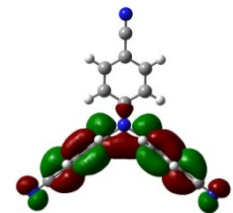
	$\lambda_{\text{trans.}}$ (nm)	Osc. strength	Major contributions
<b>mCN</b>	338.53	0.4516	HOMO→LUMO (87%)
	308.02	0.1669	HOMO→LUMO+2 (91%)
	225.50	0.0554	HOMO-5→LUMO (26%), HOMO-1→LUMO+2 (39%)
	224.59	0.0604	HOMO-3→LUMO (39%), HOMO-2→LUMO+2 (-31%)
	221.02	0.0914	HOMO-3→LUMO+1 (-26%), HOMO-1→LUMO+1 (35%), HOMO-1→LUMO+2 (25%)
	219.41	0.1655	HOMO-2→LUMO+1 (73%)
	218.25	0.0389	HOMO→LUMO+11 (87%)
<b>dCN</b>	354.02	0.4972	HOMO→LUMO (88%)
	320.87	0.2315	HOMO→LUMO+1 (88%)
	237.34	0.0443	HOMO-4→LUMO (62%), HOMO-2→LUMO+2 (12%), HOMO-1→LUMO+1 (-11%)
	234.16	0.0589	HOMO-4→LUMO (15%), HOMO-1→LUMO+1 (55%)
	233.39	0.0917	HOMO-3→LUMO (62%), HOMO-2→LUMO+1 (11%)
	220.00	0.1418	HOMO-5→LUMO+1 (-30%), HOMO-3→LUMO+1 (43%)
<b>tCN</b>	350.76	0.4188	HOMO→LUMO (89%)
	350.61	0.4204	HOMO→LUMO+1 (89%)
	237.80	0.1395	HOMO-4→LUMO+1 (-15%), HOMO-3→LUMO (-15%), HOMO-2→LUMO+2 (20%), HOMO-1→LUMO+1 (-11%)
	237.79	0.139	HOMO-4→LUMO+1 (19%), HOMO-3→LUMO (-11%), HOMO-2→LUMO+1 (-10%), HOMO-1→LUMO (12%), HOMO-1→LUMO+2 (20%)
	217.65	0.3645	HOMO-5→LUMO (15%), HOMO-3→LUMO+2 (-10%), HOMO-2→LUMO+2 (-49%)

Table S3 Energies of frontier molecular orbitals calculated at different level of theory.

Compound	Orbitals	Energy (eV)				
		B3LYP/ 6-31G	B3LYP/6- 31+G(d)	B3LYP/6- 31+G(d,p)	$\omega$ B97X/6 -31G	M062X/6 -31G
<b>mCN</b>	LUMO+2	-0.57	-1.03	-1.06	1.63	0.38
	LUMO+1	-0.71	-1.22	-1.26	1.47	0.19
	LUMO	-1.20	-1.58	-1.61	0.82	-0.27
	HOMO	-5.41	-5.71	-5.73	-7.59	-6.61
	HOMO-1	-7.02	-7.27	-7.28	-9.50	-8.44
	HOMO-2	-7.13	-7.35	-7.38	-9.77	-8.54
<b>dCN</b>	LUMO+2	-1.09	-1.61	-1.63	1.12	-0.14
	LUMO+1	-1.33	-1.71	-1.74	0.87	-0.35
	LUMO	-1.77	-2.15	-2.16	0.33	-0.84
	HOMO	-5.82	-6.12	-6.13	-7.97	-6.99
	HOMO-1	-7.40	-7.62	-7.63	-9.85	-8.79
	HOMO-2	-7.56	-7.78	-7.79	-10.04	-8.95
<b>tCN</b>	LUMO+2	-1.44	-1.96	-2.00	0.73	-0.49
	LUMO+1	-2.07	-2.45	-2.46	0.03	-1.09
	LUMO	-2.07	-2.45	-2.46	0.03	-1.09
	HOMO	-6.18	-6.48	-6.49	-8.33	-7.35
	HOMO-1	-7.81	-8.03	-8.05	-10.26	-9.22
	HOMO-2	-7.81	-8.03	-8.05	-10.29	-9.22



Table S4 Contour Plots of the pairs of “Natural Transition Orbitals” based on TD-DFT calculations at B3LYP/6-31+G(d,p) level of theory

Compound	Based on the S <sub>0</sub> State			Based on the S <sub>1</sub> State		
	NTO of hole	NTO of electron	$\lambda$	NTO of hole	NTO of electron	$\lambda$
mCN			0.99			0.99
dCN			0.99			0.99
tCN			0.99			0.99

$\lambda$  represents natural transition orbital eigenvalue

Table S5 Dipole moments of ground and excited state<sup>s1</sup> estimated from the experimental data

Sample	$m_1$	$m_2$	$a$ (A°)	$\mu_g$ (D)	$\mu_e$ (D)	$\Delta\mu$ (D)	$\mu_e/\mu_g$
mCN	5199	6553	4.46	0.93	8.1	7.2	8.7
dCN	1407	9768	4.51	11.2	15.0	3.9	1.3
tCN	2649	8167	4.63	5.6	11.0	5.3	2.0

The dipole moments were calculated using the following equations. <sup>S2</sup>

$$\nu_a - \nu_f = m_1 f(\epsilon, n) + \text{const.}$$

$$\nu_a + \nu_f = -m_2 [f(\epsilon, n) + 2g(n)] + \text{const.}$$

$$\text{where } f(\epsilon, n) = \frac{2n^2 + 1}{n^2 + 2} \left[ \frac{\epsilon - 1}{\epsilon + 2} - \frac{n^2 - 1}{n^2 + 2} \right]$$

is the polarity of the solvent [37] and

$$g(n) = \frac{3}{2} \left[ \frac{n^4 - 1}{(n^2 + 2)^2} \right]$$

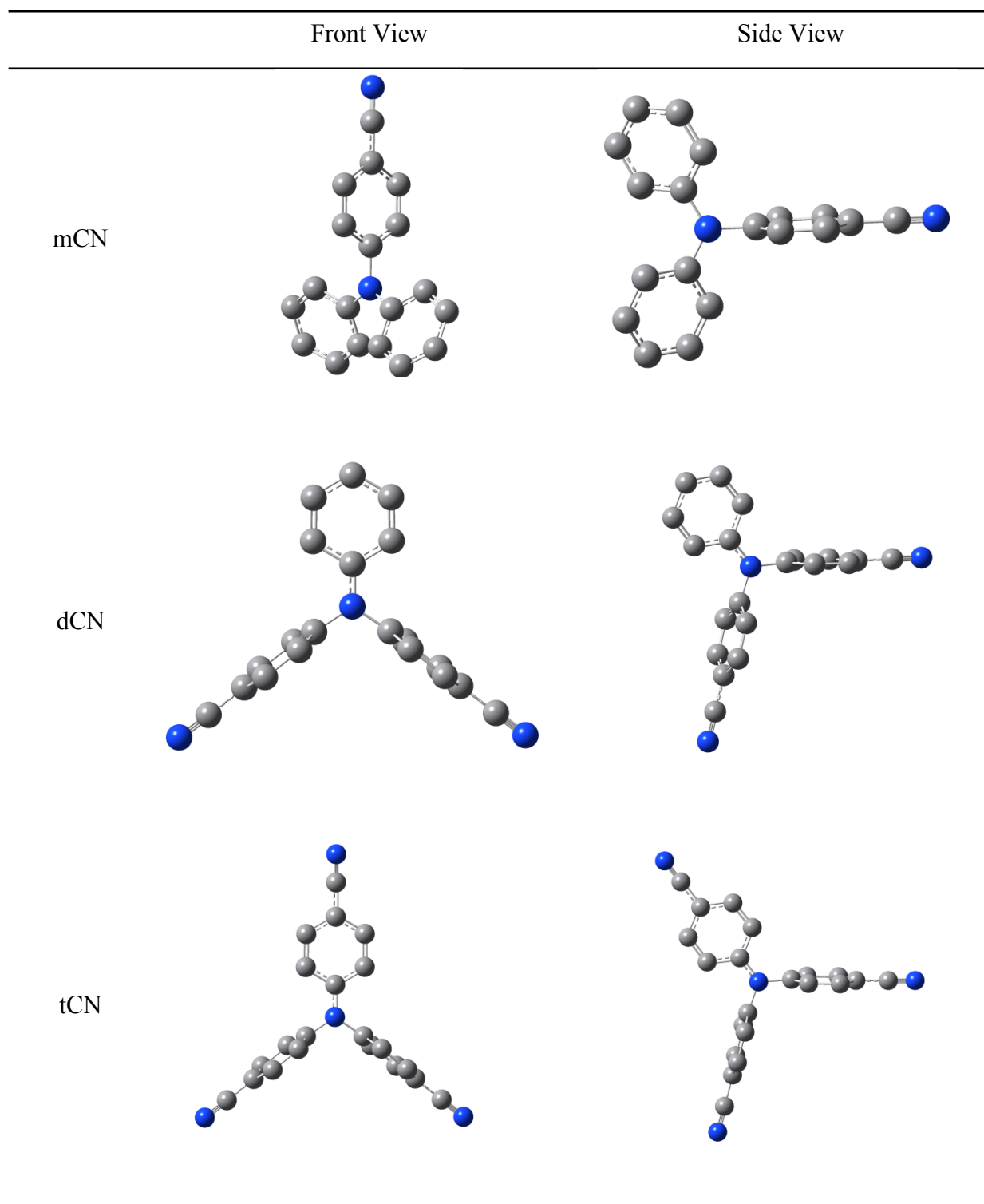
$$\text{with } m_1 = \frac{2(\mu_e - \mu_g)^2}{hca^3}$$

$$\text{and } m_2 = \frac{2(\mu_e^2 - \mu_g^2)}{hca^3}$$

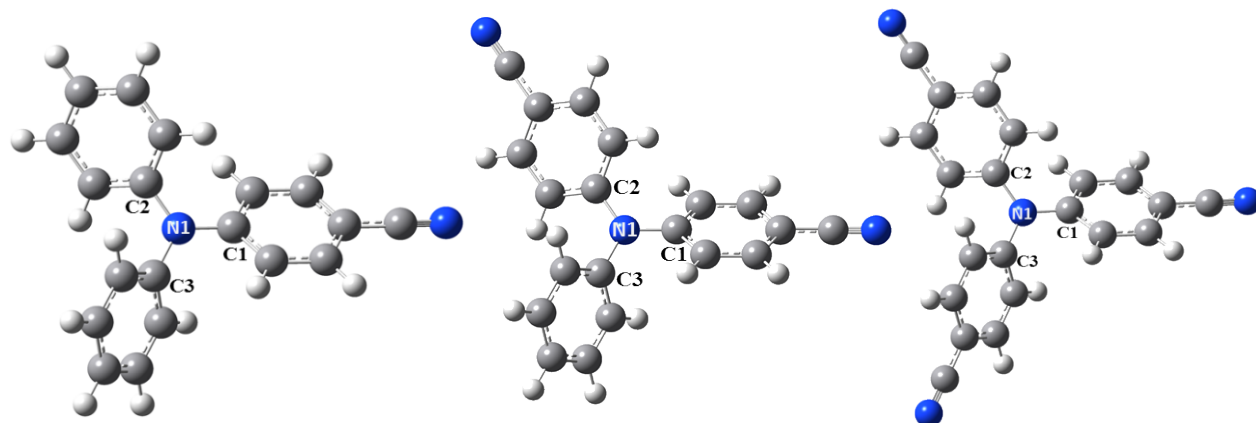
The  $m_1$  and  $m_2$  are calculated from the absorption and fluorescence spectral shifts as a function of solvent polarity parameter.  $h$ , Planck's constant  $c$ , the velocity of light in vacuum  $\nu_a$  – absorption maximum,  $\nu_b$  – fluorescence maximum, and  $n$ - refractive index.

**Table S6** Photophysical properties of cyanotriphenylamines in different solvents

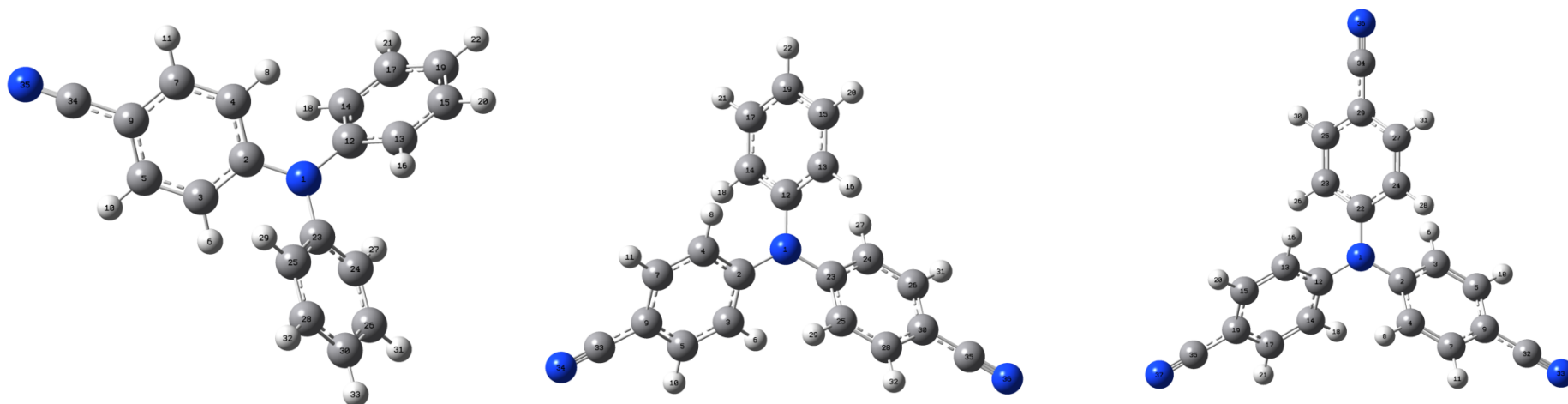
<b>Compound</b>	<b>Solvent</b>	$\lambda_{\text{abs}}$ <b>nm</b>	$\lambda_{\text{fl}}$ <b>nm</b>	<b>Stokes shift,</b> <b>cm<sup>-1</sup></b>	$\phi_{\text{f}}$	$\tau_{\text{f}}$ , ns	$k_{\text{r}}$ [10 <sup>9</sup> s <sup>-1</sup> ]	$k_{\text{nr}}$ [10 <sup>9</sup> s <sup>-1</sup> ]
<b>mCN</b>	Hexane	325	390	5128	0.16	0.59	3.7	0.73
	Toluene	330	405	4044	0.11	2.3	20.9	0.95
	Chloroform	333	430	6774	0.08	5.2	65.0	0.98
	Ethylacetate	325	428	7405	0.11	4.7	42.7	0.98
	Dichloromethane	330	433	7208	0.06	7.1	118.3	0.99
	DMSO	328	460	8749	0.06	10.0	166.7	0.99
	Acetonitrile	322	460	9317	0.05	6.3	126.0	0.99
<b>dCN</b>	Hexane	332	378	3665	0.24	1.6	6.7	0.85
	Toluene	344	387	3230	0.14	1.5	10.7	0.91
	Chloroform	350	397	3383	0.06	1.3	21.7	0.95
	Ethylacetate	344	404	4317	0.10	1.6	16.0	0.94
	Dichloromethane	350	376	1976	0.07	2.1	30.0	0.97
	DMSO	349	426	5179	0.07	3.0	42.9	0.98
	Acetonitrile	346	424	5317	0.05	2.4	48.0	0.98
<b>tCN</b>	Toluene	335	369	2750	0.15	1.3	8.7	0.88
	Chloroform	336	374	3024	0.04	1.6	40.0	0.98
	Ethylacetate	335	378	3396	0.07	1.6	22.9	0.96
	Dichloromethane	336	375	3095	0.02	1.8	90.0	0.99
	DMSO	344	404	4317	0.06	3.1	51.7	0.98
	Acetonitrile	336	399	4699	0.05	3.5	70.0	0.99

**Table S7** Optimized geometries of singlet excited state

**Table S8** Comparison between the bond lengths of ground and excited states of cyano TPA derivatives



Cmpd.	Bond Length (Å)					
	C1-N1		C2-N1		C3-N1	
	GS	ES	GS	ES	GS	ES
<b>mCN</b>	1.407	1.460	1.429	1.397	1.429	1.397
<b>dCN</b>	1.414	1.448	1.414	1.448	1.433	1.342
<b>tCN</b>	1.420	1.450	1.420	1.450	1.420	1.337

**Table S9** Comparison between the bond lengths of ground and excited states of cyano TPA derivatives

mCN			dCN			tCN		
Dihedral Angle	Ground State	Excited State	Dihedral Angle	Ground State	Excited State	Dihedral Angle	Ground State	Excited State
C25-C23-N1-C2	48°	150°	C25-C23-N1-C2	38°	87°	C4-C2-N1-C22	138°	86
C14-C12-N1-C2	48°	26°	C24-C23-N1-C2	143°	87°	C14-C12-N1-C22	138°	180
			C14-C12-N1-C2	51°	0.0°	C24-C22-N1-C2	41°	86

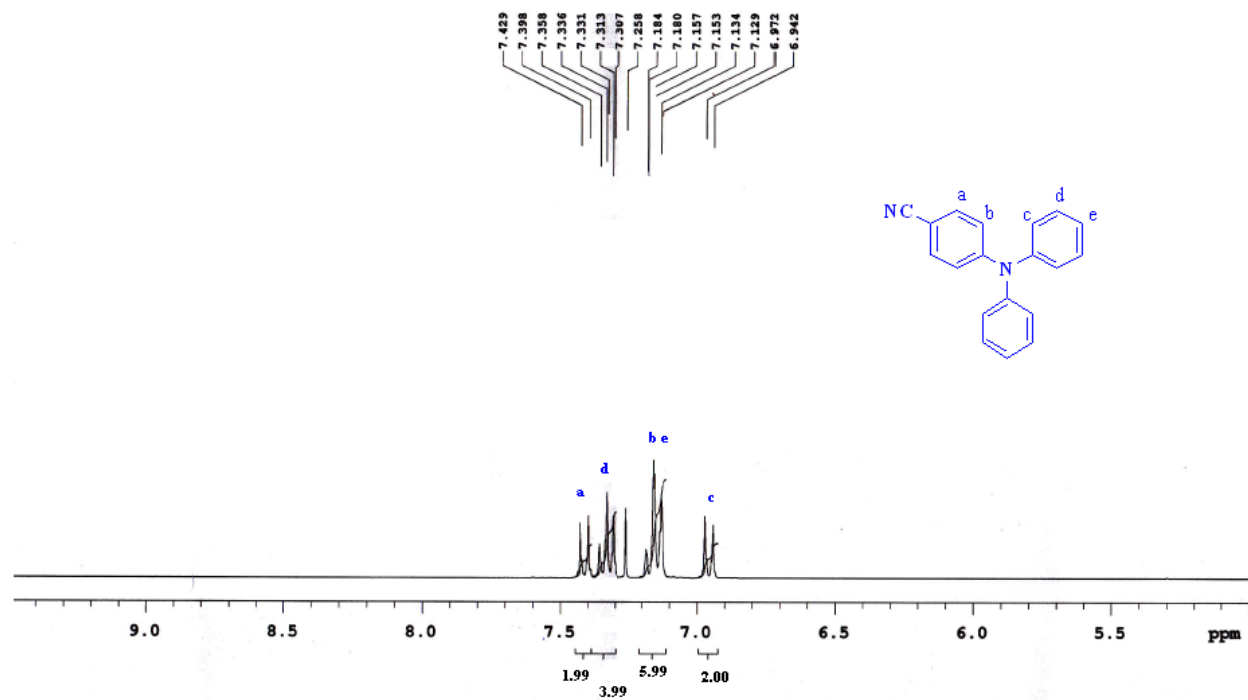


**Figure S1** <sup>1</sup>H-NMR spectrum of 4-(diphenylamino)benzonitrile

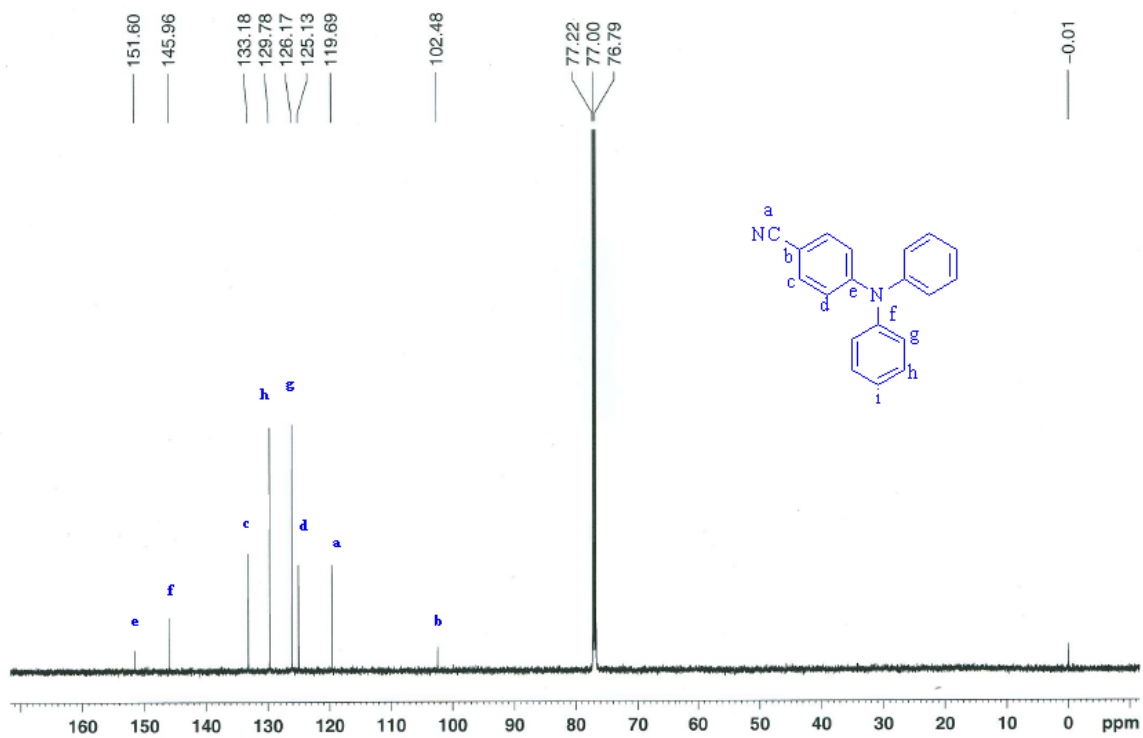


**Figure S2**  $^{13}\text{C}$ -NMR spectrum of 4-(diphenylamino)benzonitrile



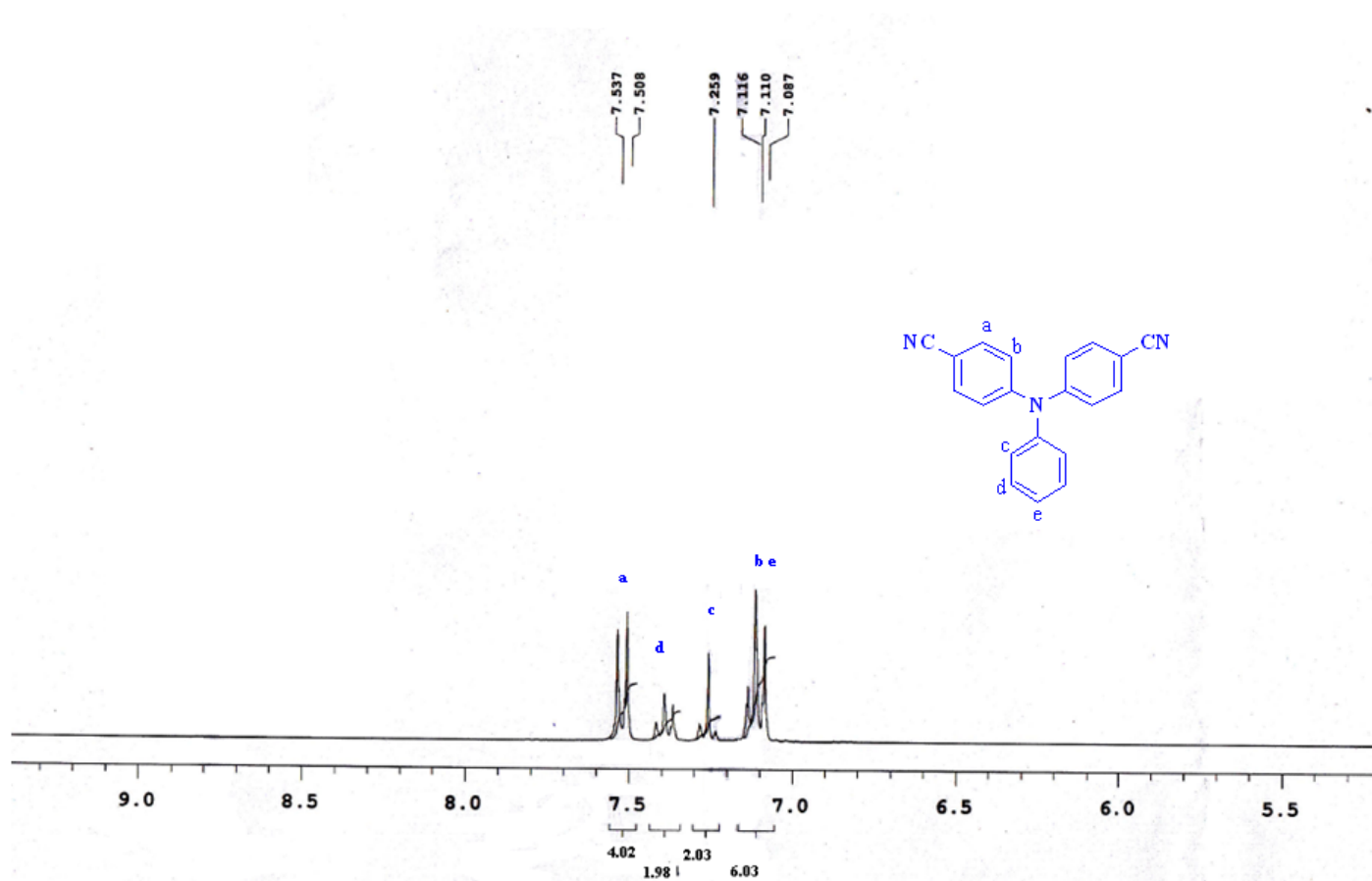


**Figure S3** <sup>1</sup>H-NMR spectrum of 4,4'-(phenylazanediyl)dibenzonitrile

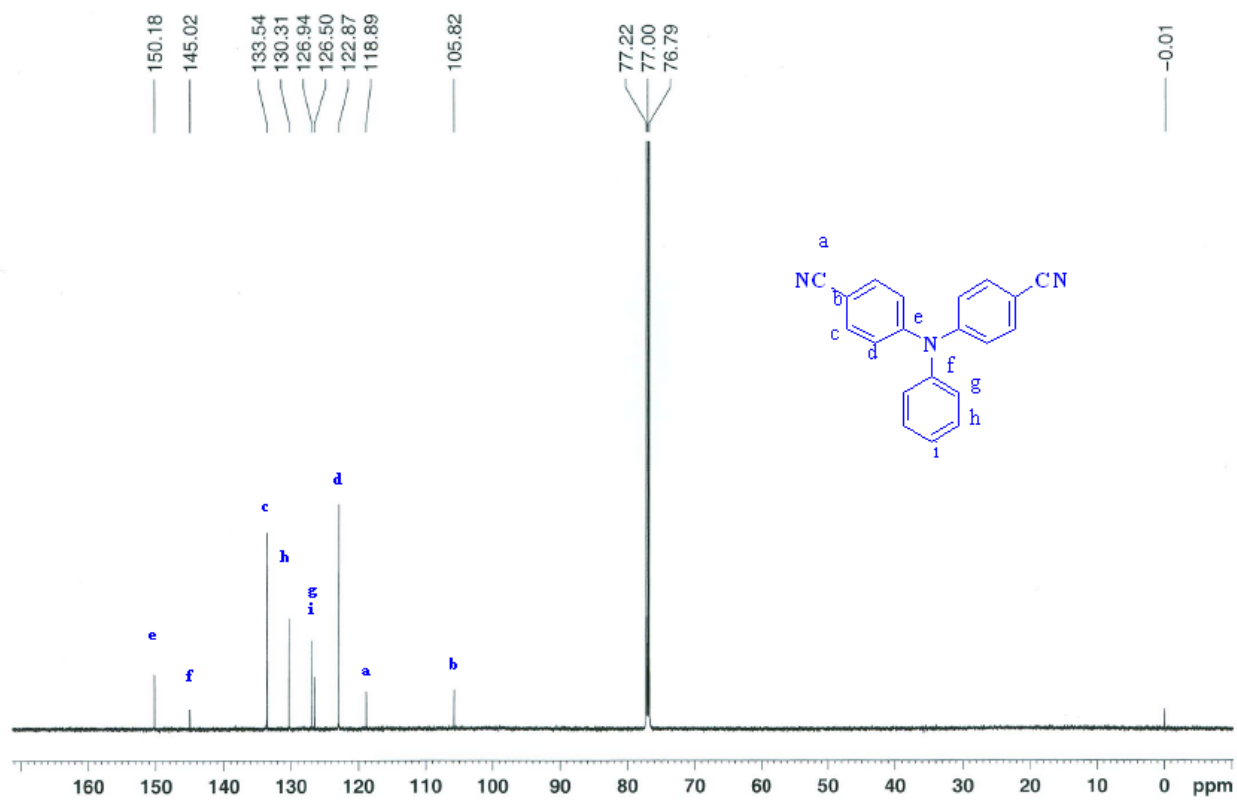


**Figure S4**  $^{13}\text{C}$ -NMR spectrum of 4,4'-(phenylazanediyl)dibenzonitrile

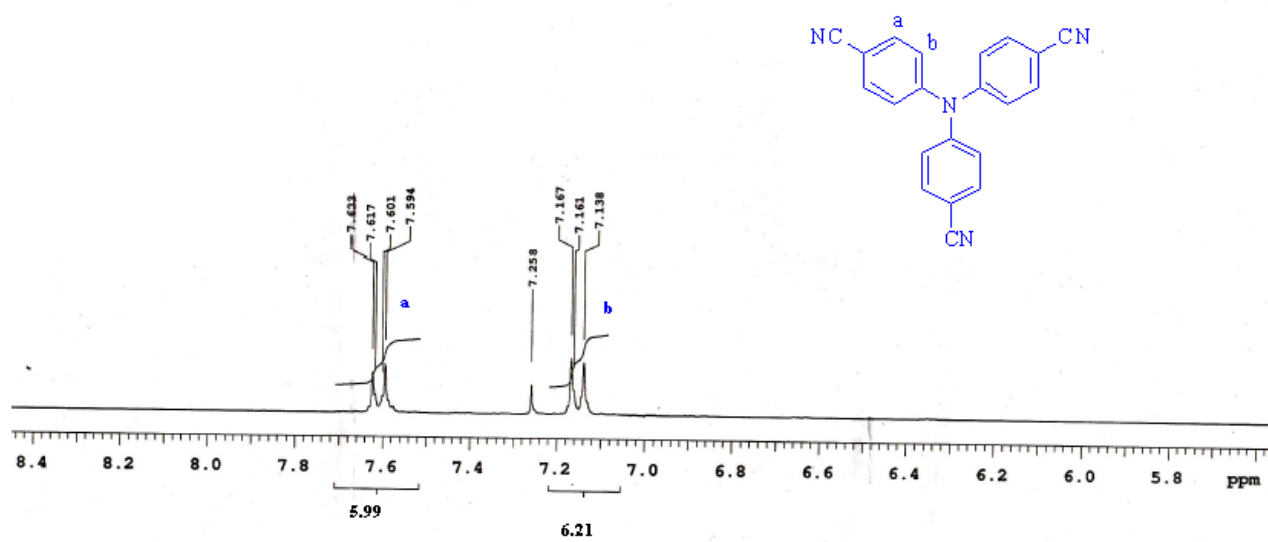


**Figure S5**  $^1\text{H-NMR}$  spectrum of 4,4',4''-nitrotribenzonitrile

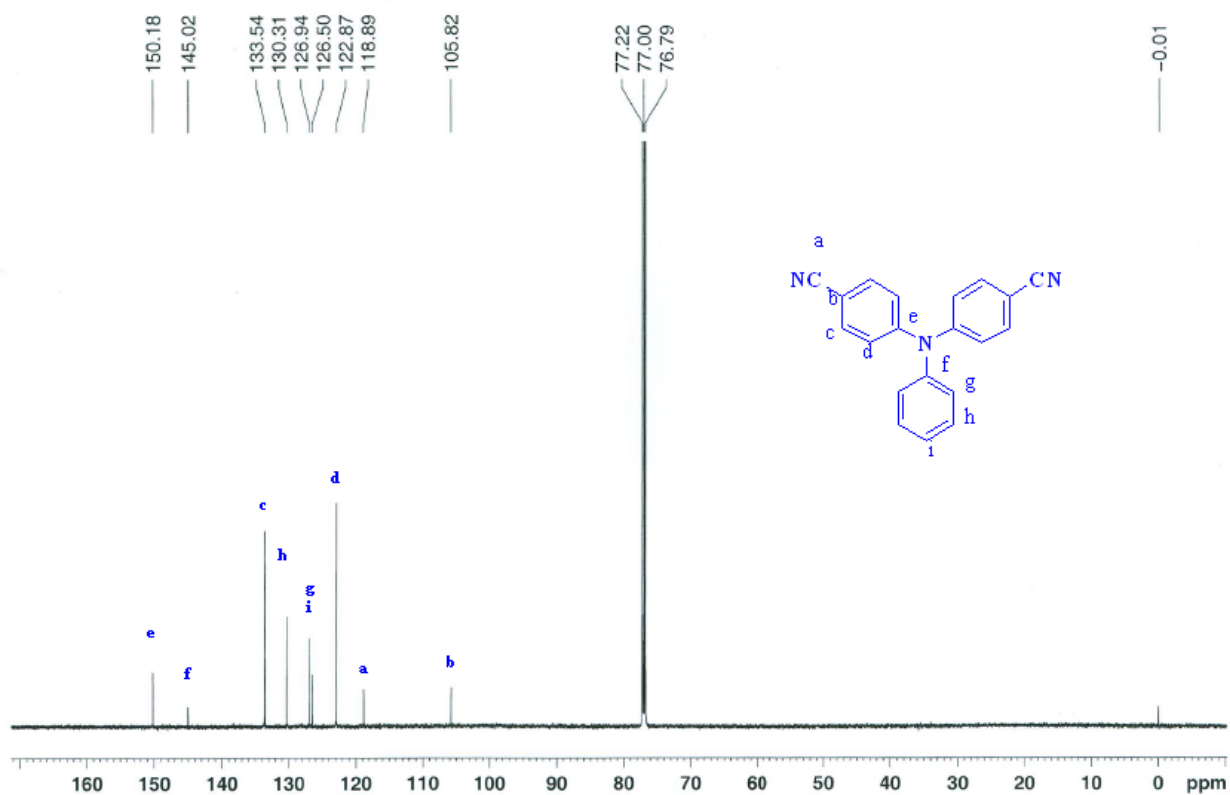


**Figure S6**  $^{13}\text{C}$ -NMR spectrum of 4,4'-(phenylazanediyl)dibenzonitrile

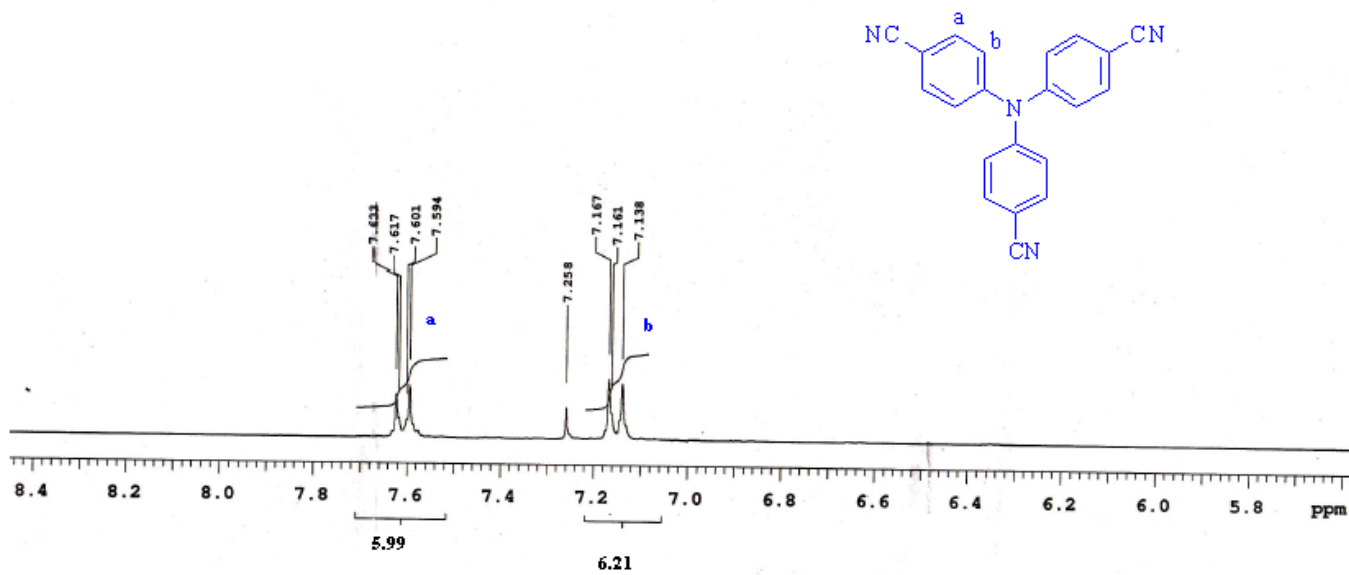


**Figure S7**  $^1\text{H-NMR}$  spectrum of 4,4',4''-nitrilotribenzonitrile

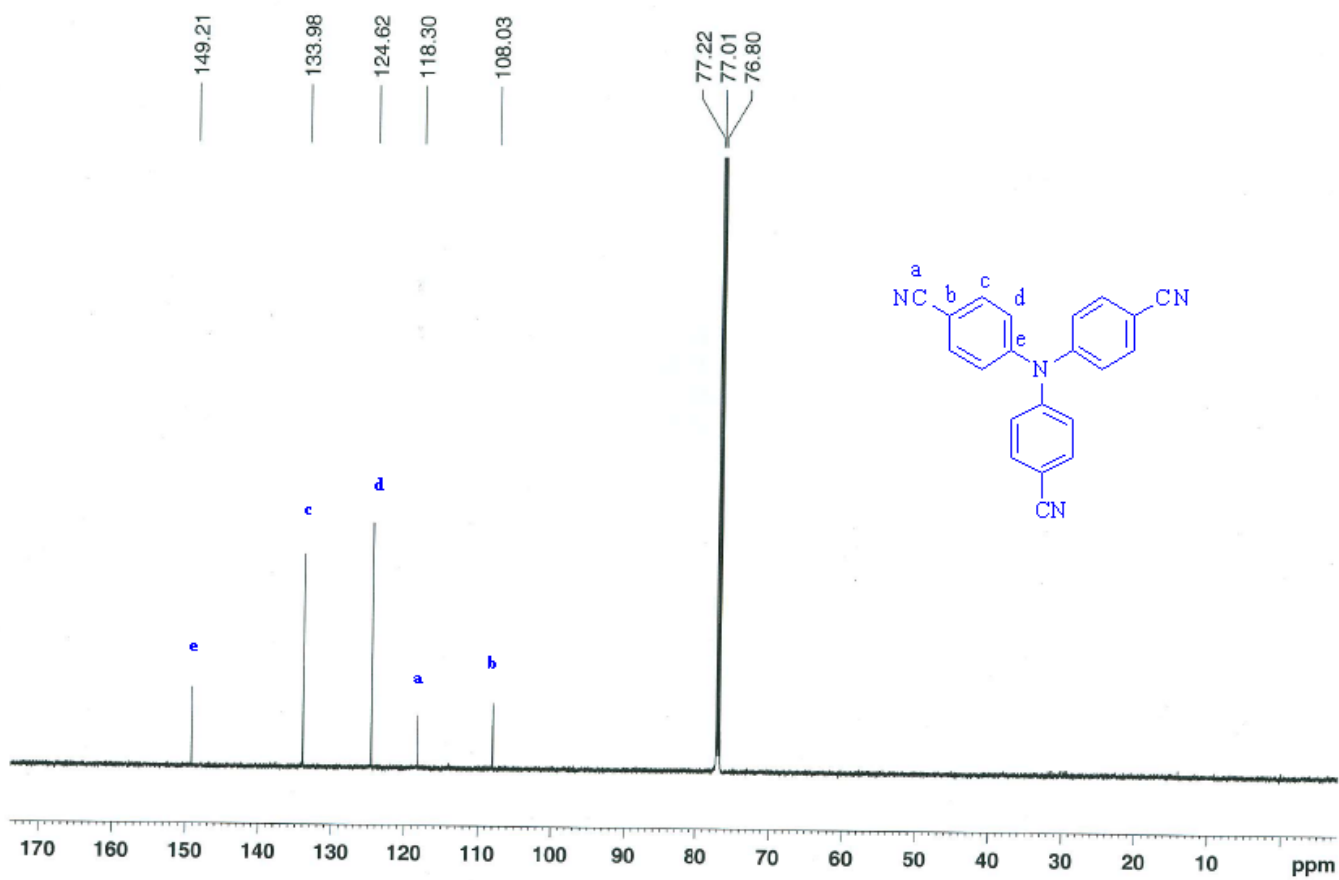


**Figure S8**  $^{13}\text{C}$ -NMR spectrum of 4,4',4''-nitrilotribenzonitrile

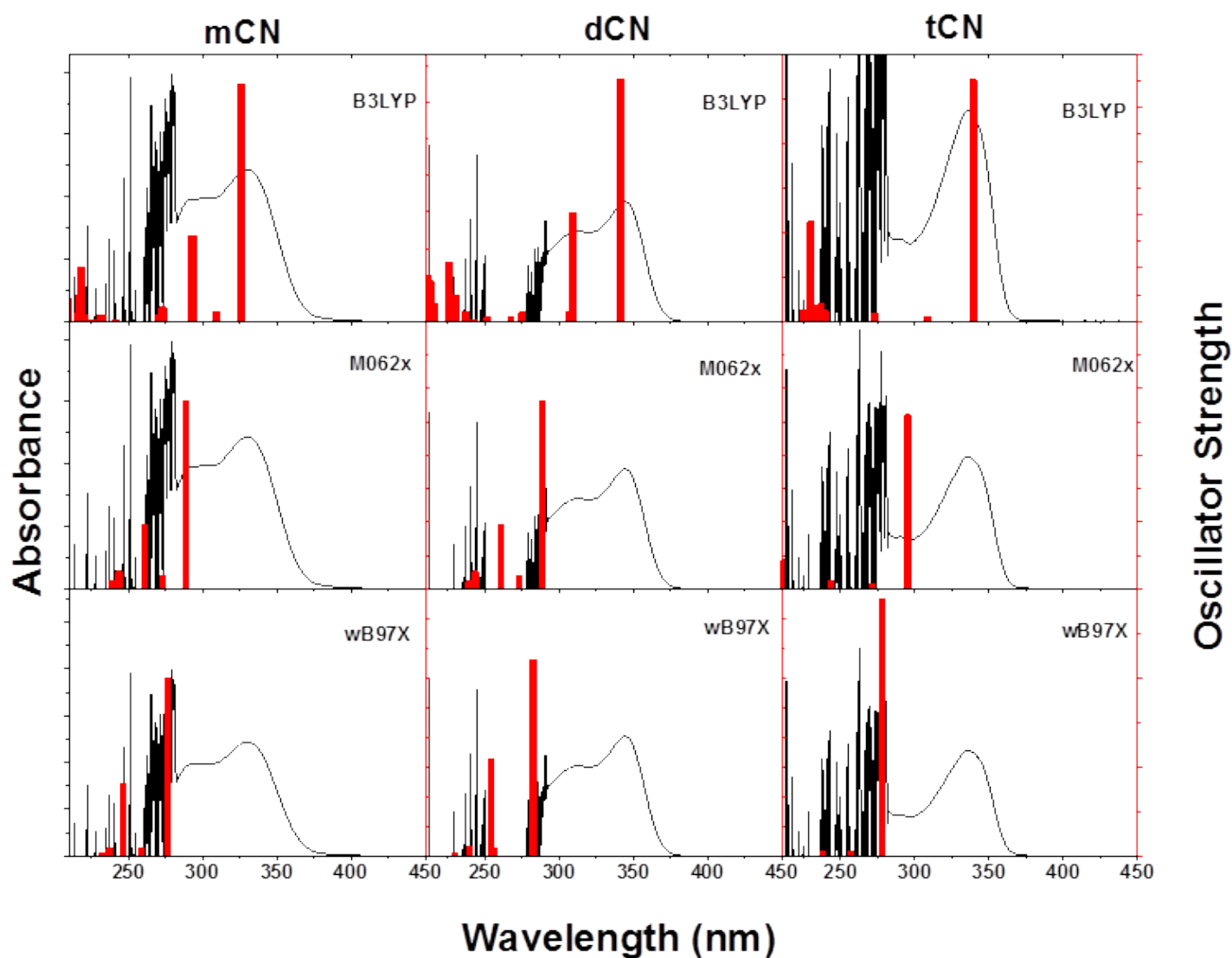


**Figure S9** Calculated (red) and experimental (black) absorption spectra of triphenylamines in toluene. The basis set employed for the calculation are given in the respective figure.

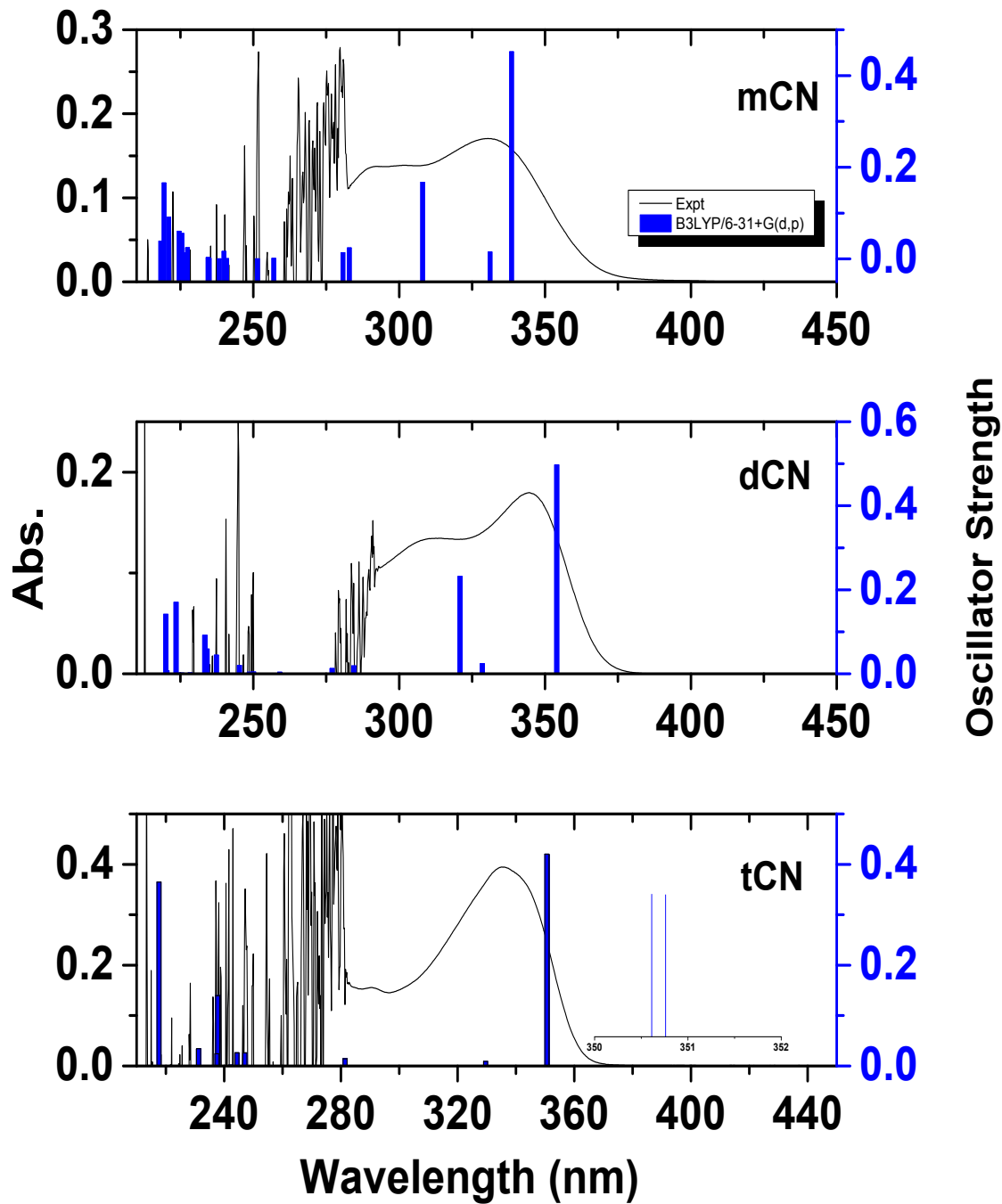


**Figure S10** Calculated (blue) and experimental (black) absorption spectra of **mCN**, **dCN**, and **tCN** in toluene. The calculations were carried at B3LYP/6-31+G(d,p) level of theory. Inset in **tCN**- Expanded region between 320-360 nm, to show the degenerate nature of the S<sub>1</sub> state.



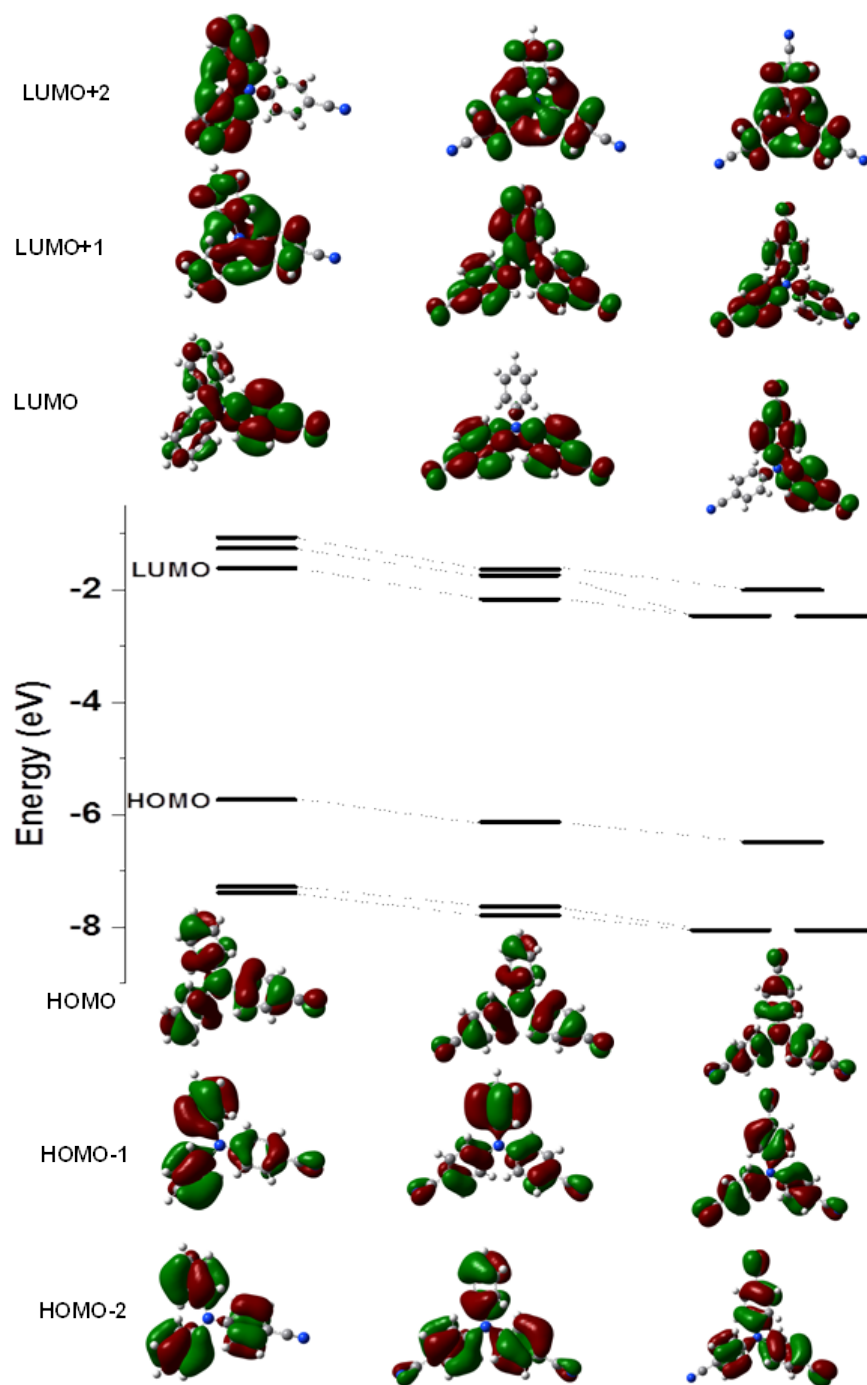


**Figure S11** Frontier molecular orbital diagram of mCN, dCN, and tCN calculated at B3LYP/6-31+G(d,p) level

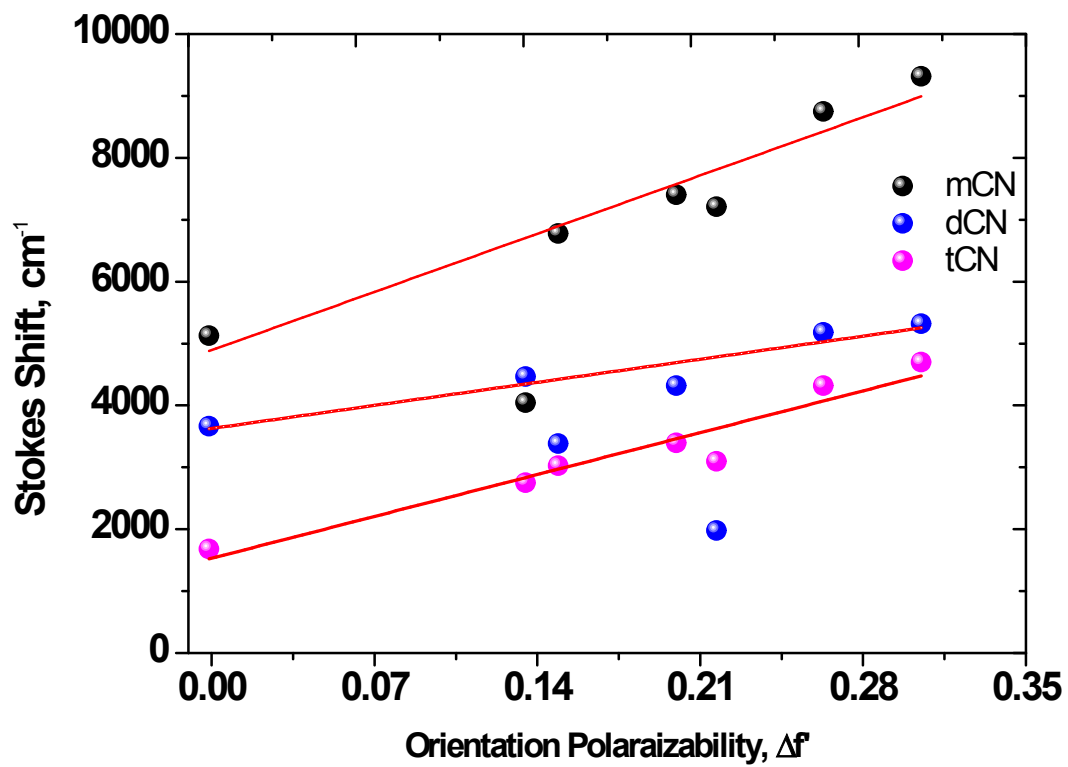
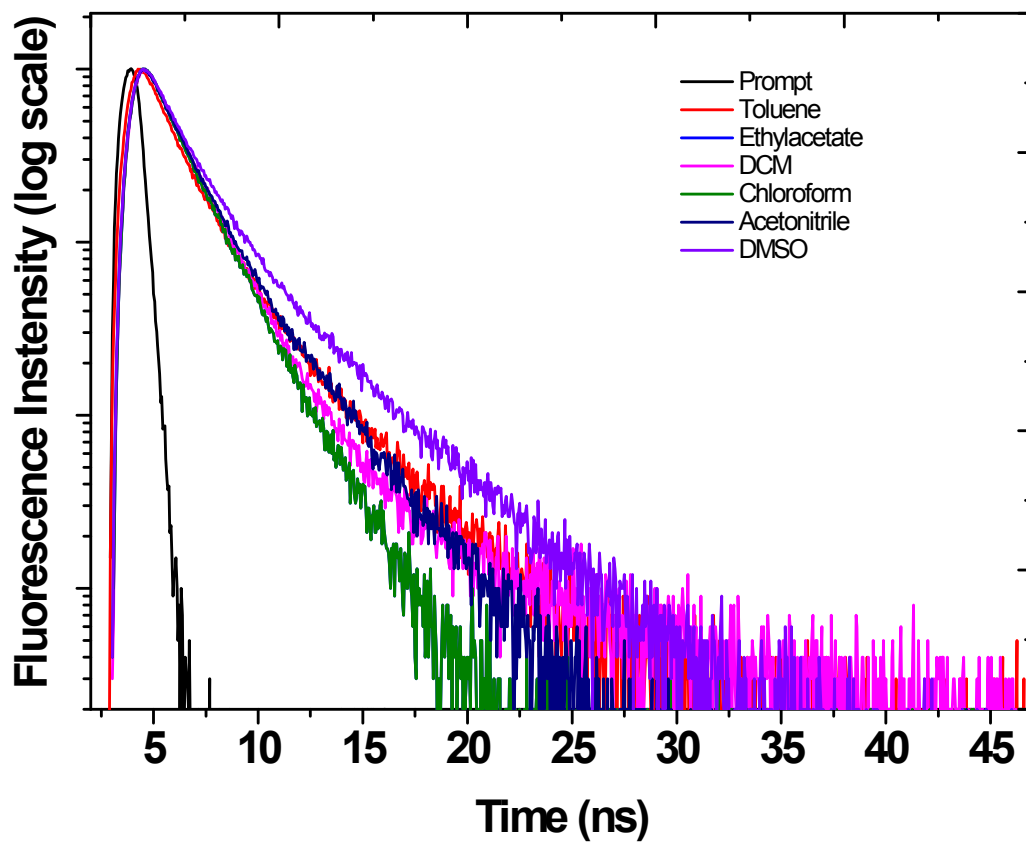
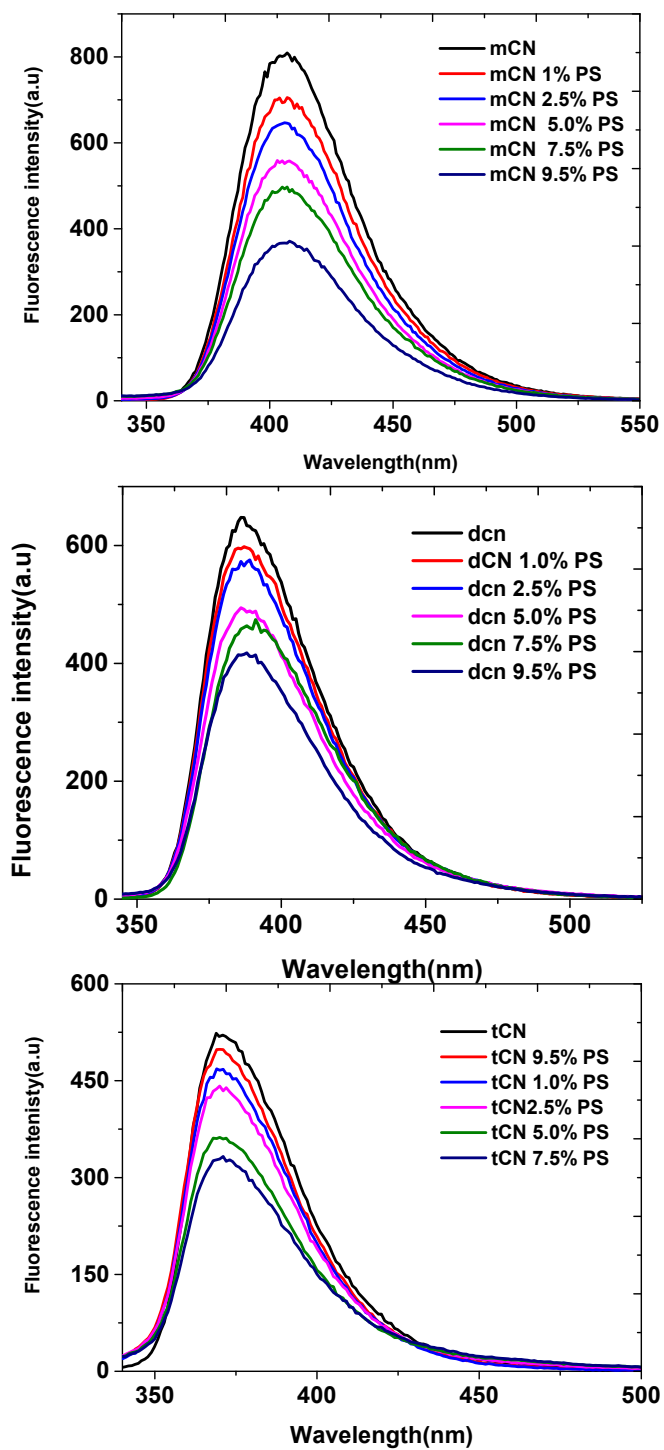


Figure S12 Lippert-mataga plot of mCN, dCN, and tCN



**Figure S13** Fluorescence decay profiles of tCN in different solvents



**Figure S14** Fluorescence spectra of cyanotriphenylamine derivatives in neat toluene and different percentages of polystyrene in toluene.

## Reference 9 with complete authors list

9. Gaussian 09, Revision C.01, M. J. Frisch, G. W. Trucks, H. B. Schlegel, G. E. Scuseria, M. A. Robb, J. R. Cheeseman, G. Scalmani, V. Barone, B. Mennucci, G. A. Petersson, H. Nakatsuji, M. Caricato, X. Li, H. P. Hratchian, A. F. Izmaylov, J. Bloino, G. Zheng, J. L. Sonnenberg, M. Hada, M. Ehara, K. Toyota, R. Fukuda, J. Hasegawa, M. Ishida, T. Nakajima, Y. Honda, O. Kitao, H. Nakai, T. Vreven, J. A. Montgomery, Jr., J. E. Peralta, F. Ogliaro, M. Bearpark, J. J. Heyd, E. Brothers, K. N. Kudin, V. N. Staroverov, R. Kobayashi, J. Normand, K. Raghavachari, A. Rendell, J. C. Burant, S. S. Iyengar, J. Tomasi, M. Cossi, N. Rega, J. M. Millam, M. Klene, J. E. Knox, J. B. Cross, V. Bakken, C. Adamo, J. Jaramillo, R. Gomperts, R. E. Stratmann, O. Yazyev, A. J. Austin, R. Cammi, C. Pomelli, J. W. Ochterski, R. L. Martin, K. Morokuma, V. G. Zakrzewski, G. A. Voth, P. Salvador, J. J. Dannenberg, S. Dapprich, A. D. Daniels, Ö. Farkas, J. B. Foresman, J. V. Ortiz, J. Cioslowski, and D. J. Fox, Gaussian, Inc., Wallingford CT, 2009.

## References

- S1 R. L. Martin, *J. Chem. Phys.* 2003, 118, 4775.
- S2. a) L. Bilot and A. Kawski, *Z. Naturforsch.*, 1962, **17a**, 621; b) L. Bilot and A. Kawski, *Z. Naturforsch.*, 1963, **18a**, 10; c) L. Bilot and A. Kawski, *Z. Naturforsch.*, 1963, **18a**, 256; d) A. Kawski, *Acta Phys. Polon.* 1966, **29**, 507; e) A. Kawski, *Progress in Photochemistry and Photophysics*, Ed. J. F. Rabek, CRC Press Boca Raton, Boston, 1992, Vol. V. pp. 1-47 and references therein.